Fabrication of Single-Crystalline Semiconductor CdS Nanobelts by Vapor Transport

Jun Zhang,* Feihong Jiang, and Lide Zhang

Department of Physics, Yantai University, Yantai, 264005, P. R. China

Received: October 1, 2003; In Final Form: March 29, 2004

A beltlike single-crystalline CdS nanostructure was successfully synthesized by vapor-phase transport of the desired commercial CdS powder at 850 °C. Its morphology and microstructures were determined by X-ray powder diffraction, scanning electron microscopy, and transmission electron microscopy. The observations reveal that the products consist of a large quantity of beltlike nanostructures with typical lengths in the range of several tens to several hundreds of micrometers. The typical widths of CdS nanobelts range from several tens to several hundreds of nanometers. The as-synthesized semiconductor CdS nanobelts are pure, structurally uniform, and single crystalline. CdS nanobelts, which have a rectangle-like cross section, could be an ideal system for building nanometer-scale optoelectronic devices along individual nanobelts, such as laser light-emitting diodes and optical devices.

Introduction

Progress in the synthesis and characterization of nanometer-scale one-dimensional structures, such as nanotubes and nanowires (nanorods), has been driven by the need to understand the novel physical properties of one-dimensional nanoscale materials in fundamental physical science and their potential application in building nanoscale electronic and optoelectronic devices.[1] Considerable effort has been made on the synthesis of nanowires or nanotubes using laser ablation,[2] template,[3] solution,[4] and other methods.[5] Recently, an important nanostructured group, which distinctly differs from hollow nanotubes and solid nanowires, has been successfully fabricated.[6−12] These nanobelts of oxides (ZnO, Ga_2O_3, SnO_2, SnO, In_2O_3, PbO_2, CdO, and MgO),[6−10] metallic Zn,[11] and semiconductor GaN[12] have a rectangular cross section with a well-defined geometry and perfect crystallinity, corresponding to a beltlike (or ribbonlike) morphology. Because of the special beltlike morphology, the nanobelts could be used for fabricating functional nanodevices and nanosize sensors based on the characteristic of individual nanobelts.

As one of the most important group II−VI semiconductors, CdS has vital optoelectronic applications for laser light-emitting diodes and optical devices based on nonlinear properties. Up to now, considerable effort has been focused on the synthesis of CdS nanowires, and the synthesis of a one-dimensional structure of CdS nanowires has been rapidly developed. For example, Routkevitch et al.[13] and Xu et al.[14] have fabricated CdS nanowires in porous anodic aluminum membranes by electrochemical deposition. Qian and co-workers have established some new chemical techniques to synthesize CdS nanowires via a solvothermal route and polymer-controlled growth.[15,16] Duan and co-workers reported that the laser-assisted catalytic growth has been developed for the synthesis of CdS nanowires.[2(a)] Wang and co-workers reported catalytic growth of large-scale single-crystalline CdS nanowires by physical evaporation.[17] Jiao and co-workers reported catalytic growth of CdS nanobelts and nanowires on tungsten substrates.[18] Due to the promising application of CdS nanowires in nanoscale optoelectronic devices, it is important to be able to synthesize these nanowires in single-crystalline form and to study their optical properties. In this communication, we report the use of the vapor-phase transport process to grow single-crystalline CdS nanobelts via a vapor−solid (VS) mechanism. Successful synthesis of II−VI group semiconductor CdS nanobelts will open up the possibility of fully studying the physical properties of nanoscale semiconductor systems, which are ideal objects for the fabrication of nanoscale functional or optoelectronic devices.

Experimental Section

Our synthesis is based on thermal evaporation of CdS powder under controlled conditions without the presence of a catalyst. High-purity CdS powder (99.99%) was used as the source. The CdS powders were put into the center of an alumina boat, and the alumina boat was covered with a quartz plate to maintain a higher CdS vapor pressure. The boat was placed in the middle of the quartz tube that was inserted in a horizontal tube furnace. Prior to heating, the system was flushed with high-purity argon (Ar) for 1 h to eliminate oxygen (O_2). Argon was introduced into the quartz tube through a mass-flow controller at the rate of 100 standard cubic centimeters per minute (sccm). Then, under a constant flow of Ar, the temperature of the furnace was rapidly increased to 850 °C from room temperature (several minutes) and was kept at 850 °C for 2 h under a constant flow of a Ar gas. After the furnace was cooled to room temperature, the argon flow was turned off. It was observed that yellow wool-like products were found on the inner wall of the alumina boat downstream.

The as-prepared products were characterized and analyzed by X-ray diffraction (XRD) (Philips PW 1710 with Cu Kα radiation), scanning electron microscopy (SEM) (JEOL JSM-5610LV), transmission electron microscopy (TEM) (Hitachi, H-800 at 200 kV), high-resolution transmission electron microscopy (HRTEM) (JEOL 2010 at 200 kV), and energy-dispersive X-ray spectroscopy (EDS) (JEOL EX-54145 JMH) attached to the SEM instrument. For HRTEM observation, the synthesized products were ultrasonically dispersed in ethanol, and a drop of the solution was then placed on a Cu grid coated

* Corresponding author. E-mail: jzhang@ytu.edu.cn.

10.1021/jp036945v CCC: $27.50
Published on Web 05/04/2004

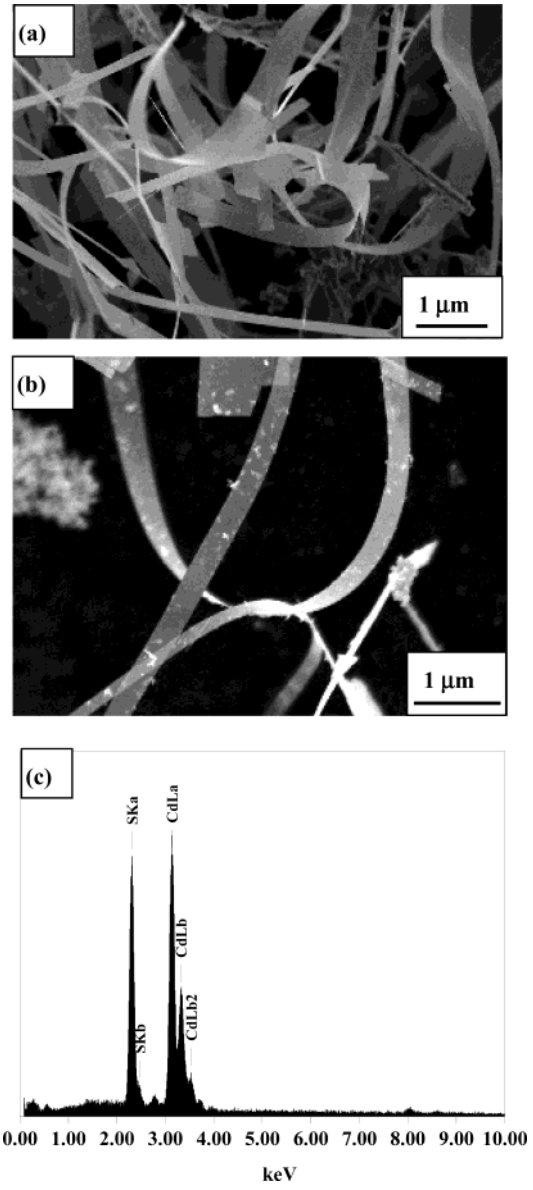

Figure 1. (a) SEM image of the as-synthesized products obtained from vapor-phase transport of CdS powder. (b) A typical high-magnification SEM image of the beltlike morphology characteristic of the nanobelts (c) EDS of an individual CdS nanobelt.

with a holey carbon film. At room temperature, Raman spectra were obtained by illuminating the sample with the 514.5 nm line of an Ar^+ laser and 1 mW output power of a laser Raman scattering spectrometer (LABRAM-HR, JY, France). Spectra of the CdS nanobelt-structure are in the frequency range between 100 and 1000 cm^{-1}, and spectral resolution is 1.0 cm^{-1}.

Results and Discussion

SEM observation shown in Figure 1(a) reveals that the products consist of a large quantity of beltlike nanostructures with typical lengths in the range of several tens to several hundreds of micrometers; some of them even have lengths on the order of millimeter. A typical magnified SEM image of the as-prepared products is given in Figure 1(b). The beltlike shape is further verified by the SEM image. The typical widths of the nanobelts are in the range of several tens to several hundreds of nanometers. Each nanobelt is uniform in width and thickness. EDS measurements [shown in Figure 1(c)] made on an individual CdS nanobelt indicate that the belt is composed of

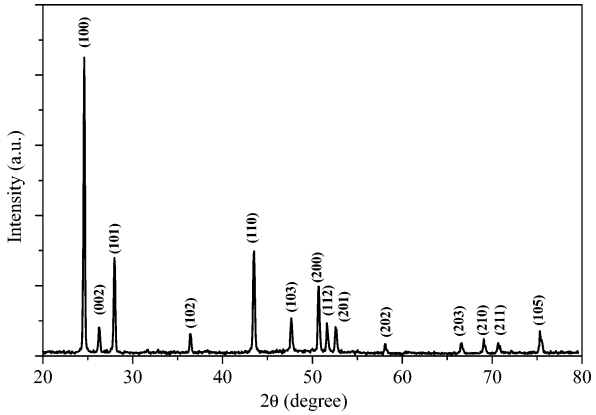

Figure 2. XRD pattern recorded from the CdS nanobelts.

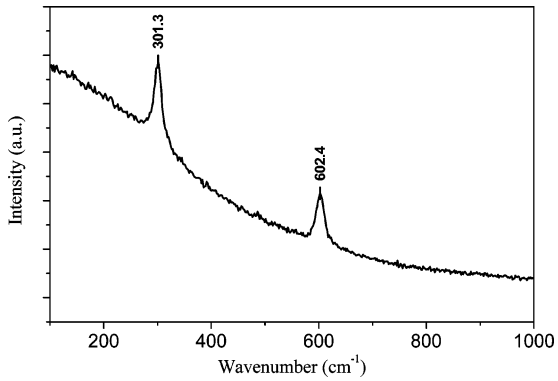

Figure 3. Raman spectrum of the CdS nanobelts at room temperature.

Cd and S. The molecular ratio of Cd/S of the nanobelt calculated from the EDS quantitative analysis data is close to that of a bulk CdS crystal.

The XRD pattern of the products shown in Figure 2 reveals the overall crystal structure of the nanobelts. Miller indices are indicated on each diffraction peak. It can be seen that the whole spectrum can be indexed in peak positions to a hexagonal wurtzite-structured CdS. The lattice constants of the crystalline phase are $a = 0.413$ nm, and $c = 0.671$ nm, consistent with the standard values for bulk CdS (JCPDS 6-314).[19] In addition, no diffraction peaks from CdO, Cd, S, or other impurities have been found in the synthesized products.

Raman spectroscopy has been proven to be a powerful tool for the investigation of material properties such as doping concentration, lattice defect identification, or crystal orientation. Figure 3 shows the Raman spectrum of the CdS nanobelts. Two features of CdS are clearly evident as shown in the figure. The Raman spectrum of the CdS nanobelts shows characteristic Raman shifts analogous to those of pure crystalline CdS.[20] The Raman peaks located at around 301.3 and 602.4 cm^{-1}. The peaks at 301.3 and 602.4 cm^{-1} agree to the first-order and second-order transverse optical (TO) phonon modes of the hexagonal CdS, respectively.

Further structural and elemental analyses of the CdS nanobelts were performed using TEM. The TEM image shown in Figure 4(a) reveals that the geometrical shape of the CdS nanostructures is a belt that is distinct in cross section from the previously reported nanotubes and nanowires. Each nanobelt has a uniform width along its entire length, and the typical widths of the nanobelts are in the range of 20 to 400 nm. A long and straight individual CdS nanobelt is displayed in Figure 4(b). The inset in the bottom-right-hand corner of Figure 4(b) is a selected area electron diffraction pattern (SAED) of the nanobelt. The SAED patterns were recorded with an electron beam perpendicular to

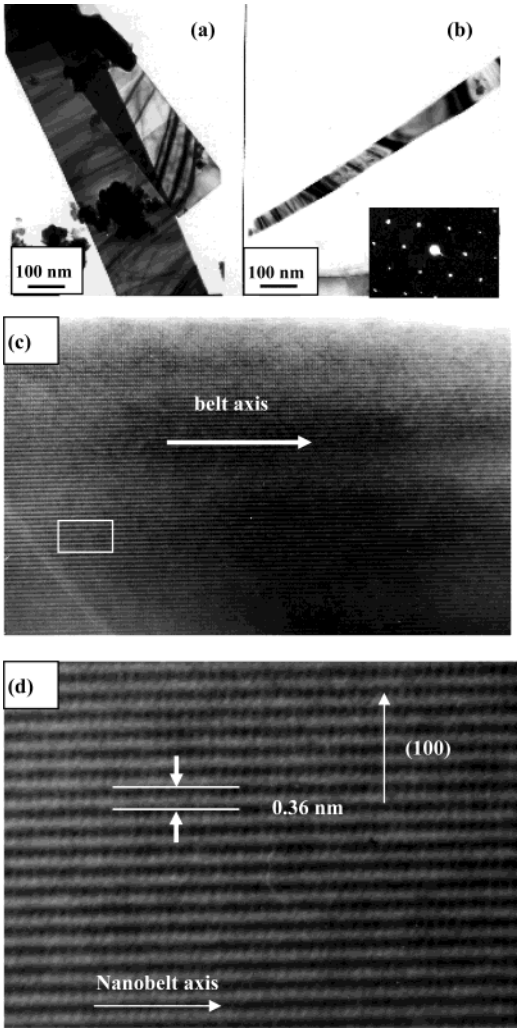

Figure 4. (a) A TEM image of two straight CdS nanobelts. (b) A TEM image of an individual CdS nanobelt. The inset in the bottom-right-hand corner shows the SAED pattern of the nanobelt. (c) HRTEM image of another CdS nanobelt, showing a clean and structurally perfect surface. The image reveals that the nanobelt is single-crystalline, no defect, and no dislocation. The surfaces of the nanobelts are clean, atomically sharp, and unsheathed amorphous phase. An arrow indicates the long axis of the nanobelt. (d) An enlargement HRTEM image of the boxed region in Figure 4(c). In this image, the space of about 0.36 nm between arrowheads corresponds to the distance between (100) planes. The {100} lattice fringes with lattice spacing around 0.36 nm are parallel to the long axis of the nanobelt.

the long axis of the nanobelt. The SAED patterns are essentially identified over the entire nanobelt, indicating the single-crystalline character of the CdS nanobelt. No particle was observed at the ends of the nanobelts. The ripplelike strain contrast can be seen in CdS nanobelts [Figure 4(a) and 4(b)]. The ripplelike contrast observed in the TEM images is due to strain resulting from the bending of the belt.

The HRTEM image [shown in Figure 4(c)] of another CdS nanobelt shows a clean and structurally perfect surface. The clear lattice fringes in the HRTEM image indicates a single-crystal structure of the nanobelt, and shows no defect and no dislocation. The surfaces of the nanobelts are clean, atomically sharp, and unsheathed amorphous phase. The axis of the CdS nanobelt is indicated by an arrow. To display further the lattice fringes of the HRTEM image, the lattice fringes are verified by an enlargement of the boxed region in Figure 4(c) as redisplayed in Figure 4(d). In this image, the spacing of about 0.36 nm between arrowheads corresponds to the distance between (100) planes. The image reveals that the {100} lattice fringes with lattice spacing around 0.36 nm are parallel to the long axis of the nanobelt. Therefore, these data from XRD, TEM, HRTEM, and EDS analyses altogether show that the products are large quantities of ultralong and single-crystalline CdS nanobelts.

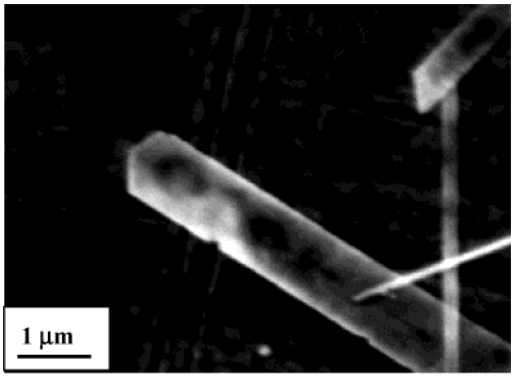

Figure 5. A SEM image of a triangle tip of an individual CdS nanobelt.

There are several possible models for the growth of conventional crystal whiskers or nanowires, dislocation, vapor−liquid−solid (VLS), solution−liquid−solid (SLS), and an oxide-assisted mechanism. However, none of the above mechanisms seems suitable to account for the growth of the CdS nanobelts. In our vapor-phase transport experiment, neither metal was employed as a catalyst, and no ball of catalyst was observed on the tip of any nanobelts (see Figure 5). TEM and SEM analyses altogether reveal that the growth of the CdS nanobelts may not be dominated by the VLS process [21] proposed for the nanowires grown by a catalytic-assisted technique.[2(a),21,22] The VLS mechanism could be ruled out. The SLS mechanism is also impossible because no solution phase was used in the experiments, and the oxide-assisted mechanism is less likely because the experiments were performed in an argon atmosphere. In addition, no evidence of dislocations was found in our observation. Therefore, it is likely that the CdS nanobelts follow a growth mechanism similar to the vapor−solid (VS) mechanism.[6−11] Because the only source material used in our synthesis is pure CdS powders and the composition of the CdS nanobelts is similar or identical to the starting material, it is likely that the growth is governed by a VS process. The typical SEM image as shown in Figure 5, which is the triangle tip of a CdS nanobelt, would be related with such growth direction. As for the VS mechanism, it is very typical that the nanowire decreases in thickness during growth and possesses a sharp tip, which is usually accepted as an indication of the growth of nanowires via the VS mechanism. In our work, the nanobelts are uniform along the whole length [see SEM images in Figure 1(b) and Figure 5, TEM image in Figure 4(a)], and no metal particle attachment is observed on the tip of the nanobelt. The whole process could be described as follows: the CdS vapor is rapidly generated at relatively high temperature for the fast heating speed by vaporizing the CdS powders. Then CdS is continuously deposited on the wall of the crucible tube downstream at lower temperatures and grows into beltlike nanostructures. On the basis of the former research results[6−11] and our experimental observations, the growth of CdS nanobelts by the vapor transport of CdS powders in this work via the VS mechanism is possible.

Conclusions

In summary, large-scale fabrication of single-crystalline CdS nanobelts was achieved through vapor-phase transport. The SEM

images show that the CdS exhibits a belt-like morphology with lengths in the range of several tens to several hundreds of micrometers, and with widths in the range of several tens to several hundreds of nanometers. The TEM images of the as-prepared nanobelts show that the nanobelts are pure, structurally uniform, and single-crystalline. XRD, Raman, and EDS analysis show that the products are large quantities of CdS nanobelts. Because of the special beltlike morphology, the optoelectronic nanodevices and nanosize sensors may be fabricated along the individual CdS nanobelts.

Acknowledgment. This work was supported by the National Natural Science Foundation of China (Grant No. 60277023).

References and Notes

(1) Hu, J. T.; Odom, T. W.; Lieber, C. M. *Acc. Chem. Res.* **1999**, *32*, 435.

(2) (a) Duan, X. F.; Lieber, C. M. *Adv. Mater*, **2000**, 12, 298. (b) Morales, A. M.; Lieber, C. M. *Science* **1998**, *279*, 208. (c) Zhang, Y.; Suenaga, K.; Colliesx, C.; Iijima, S. *Science* **1998**, *281*, 973.

(3) (a) Huang, M. H.; Choudry, A.; Yang, P.; *Chem. Commun.* **2000**, *12*, 1603. (b) Zhu, J.; Fan, S. *J. Mater Res.* **1999**, *14*, 1175.

(4) Holmes, J. D.; Johnston, K. P.; Doty, C. R.; Korgel, B. A. *Science* **2000**, *287*, 1471.

(5) (a) Wu, Y. Y.; Yang, P. D. *Chem. Mater*. **2000**, *12*, 605. (b) Bai, Z. G.; Yu, D. P.; Zhang, H. Z.; Ding, Y.; Wang, Y. P.; Gai, X. Y.; Hang, Q. L.; Xiong, G. C.; Feng, S. Q.; *Chem. Phys. Lett.* **1999**, *303*, 311. (c) Yu, D. P.; Bai, Z. G.; Ding, Y.; Hang, Q. L.; Zhang, H. Z.; Zou, Y. H.; Wang, J. J.; Qian, W.; Zhou, H. T.; Xing, G. E.; Feng, S. A. *Appl. Phys. Lett.* **1998**, *72*, 3458. (d) Tenne, R.; Margulis, L.; Genut, M.; Hodes, G. *Nature* **1992**, *360*, 444.

(6) Pan, Z. W.; Dai, Z. R.; Wang, Z. L. *Science* **2001**, *291*, 1947.

(7) Dai, Z. R.; Pan, Z. W.; Wang, Z. L. *J. Phys. Chem. B* **2002**, *106*, 902.

(8) Pan, Z. W.; Dai, Z. R.; Wang, Z. L. *Appl. Phys. Lett.* **2001**, *80*, 309.

(9) Wang, Z. L.; Pan, Z. W. *Adv. Mater*. **2002**, *14*, 1029.

(10) Zhang, J.; Zhang, L. D. *Chem. Phys. Lett.* **2002**, *363*, 293.

(11) Wang, Y. W.; Zhang, L. D.; Meng, G. W.; Liang, C. H.; Wang, G. Z.; Sun, S. H. *Chem. Commun.* **2001**, *24*, 2632.

(12) Bae, S. Y.; Seo, H. W.; Park, J. *Appl. Phys. Lett.* **2002**, *81*, 126.

(13) Routkevitch, D.; Bigioni, T.; Moskovits, M.; Xu, J. M. *J. Phys. Chem.* **1996**, *100*, 14037.

(14) Xu, D. S.; Xu, Y. J.; Chem, D. P.; Guo, G. L.; Gui, L. L.; Tang, Y. Q. *Adv. Mater.* **2000**, *12*, 520.

(15) Yang, J.; Zeng, J. H.; Yu, S. H.; Yang, L.; Zhou, G. E.; Qian, Y. T. *Chem. Mater*. **2000**, *12*, 3259.

(16) Li, Y. D.; Liao, H. W.; Ding, Y.; Qian, Y. T.; Yang, L.; Zhou, G. E. *Chem. Mater*. **1998**, *10*, 2301.

(17) Wang, Y. W.; Meng, G. W.; Zhang, L. D.; Liang, C. H.; Zhang, J. *Chem. Mater.* **2002**, *14*, 1773.

(18) Dong, L.; Jiao, J.; Coulter, M.; Love, L. *Chem. Phys. Lett.* **2003**, *376*, 653.

(19) Powder Diffraction File. Inorganic Vol. No. PD1S-SiRB, 6-314 file. Published by the Joint Committee on Powder Diffraction Standards USA, 1601 Park Lane, Swarthmore, PA 19081.

(20) Suh, J. S.; Lee, J. S. *Chem. Phys. Lett.* **1997**, *281*, 384.

(21) Wagner, R. S.; Ellis, W. C. *Appl. Phys. Lett.* **1964**, *4*, 89.

(22) Duan, X. F.; Huang, Y.; Cui, Y.; Wang, J.; Lieber, C. M. *Nature* **2001**, *409*, 66.